Optics Letters

Resonance-enhanced high harmonic in metal ions driven by elliptically polarized laser pulses

Yu Hang Lai,[1,2,*] Konda Srinivasa Rao,[1] Jingguang Liang,[1,2] Xu Wang,[3,5] Chunlei Guo,[4] Weili Yu,[1,2,6] and Wei Li[1,2]

[1]GPL, State Key Laboratory of Applied Optics, Changchun Institute of Optics, Fine Mechanics and Physics, Chinese Academy of Sciences, Changchun 130033, China
[2]University of Chinese Academy of Sciences, Beijing 100049, China
[3]Graduate School, China Academy of Engineering Physics, Beijing 100193, China
[4]The Institute of Optics, University of Rochester, Rochester, New York 14627, USA
[5]e-mail: xwang@gscaep.ac.cn
[6]e-mail: weiliyu@ciomp.ac.cn
*Corresponding author: laiyh@ciomp.ac.cn

Received 18 March 2021; revised 8 April 2021; accepted 15 April 2021; posted 16 April 2021 (Doc. ID 425495); published 6 May 2021

Resonance enhancement of a single order harmonic has been a main attractive feature in high-harmonic generation from laser ablated plumes of metals. Although it has been extensively investigated experimentally and theoretically, studies so far have focused only on linearly polarized driving fields. In this Letter, we study the dependence of the resonant harmonic yield in tin ions on the driving laser ellipticity. We find that the resonance leads to a less rapid decay of the harmonic yield as a function of driving ellipticity, and it is qualitatively reproduced by quantum mechanical simulations. To the best of our knowledge, our findings provide a new type of evidence for supporting previously proposed mechanisms for enhancement.

https://doi.org/10.1364/OL.425495

High-harmonic generation (HHG) is a highly non-perturbative phenomenon that can be used to generate coherent, ultrashort extreme-ultraviolet (XUV) pulses. It has found important applications in ultrafast science (for a review, see, e.g., [1]). Although the essential process of HHG can be intuitively understood by considering the semi-classical laser-driven motion of the freed electron from an atom [2], properly incorporating quantum effects due to atomic (or ionic) resonances into the picture is critical for explaining numerous important experimental features. However, accurately identifying the role of resonances in HHG or other strong-field processes has been challenging. A main complication is that atomic level structures can be significantly disturbed by an intense field, and so the resonance processes may be altered. Also, in the regime of tunnel ionization, the process of electron tunneling into the continuum dominates, and so the contribution of a bound–bound transition may not be readily observable. Nevertheless, resonance enhancement effects in HHG are of particular interest, due not only to fundamental importance, but also because these effects might be exploited to boost harmonic conversion efficiencies, which are inherently low. For instance, Paul *et al.* [3] found that harmonic yields from rubidium atoms could be drastically enhanced if they were resonantly pre-excited. Yuan *et al.* found that HHG from argon atoms could also be enhanced by pre-excitation [4]. Rothhardt *et al.* [5] observed a narrowband enhancement due to Fano resonance in HHG of argon. Broadband enhancements due to giant autoionization resonances in xenon [6] and manganese atoms [7] have also been reported.

Perhaps so far the most robust and readily visible type of resonant HHG phenomenon is the order-of-magnitude enhancement of a single order harmonic in several kinds of transition metal ions in laser ablated plumes [8–10]. The existence of this type of enhancement appears to be relatively insensitive to the variations of medium density, laser intensity, and pulse duration. The mechanism of this kind of enhancement has been investigated both experimentally and theoretically. At first, it was unclear whether it was well explained from just the single-atom resonance response or necessary to consider how the resonance actually affects the macroscopic plasma dispersion properties that lead to favorable phase matching conditions for the harmonics at specific frequencies [11–13]. So far, several experiments [14–16] indicate that macroscopic dispersion properties do not seem to play a decisive role in the existence of enhanced harmonics. On the other hand, several theoretical models [13,17–19] based on a single-atom response have been presented. In particular, the "four-step" model proposed by Strelkov [18] provided a clear physical picture for the process. In that model, the returning electron does not directly recombine to the ground state as in the commonly used "three-step" model; instead, it is recaptured at an autoionizing state and subsequently transits back to the ground state by the emission of a photon. Single-active electron time-dependent Schrödinger equation (TDSE) calculation incorporating the model potential in [18] and the analytical theory based on the model [20] were shown to reproduce the intensity enhancement and large phase shift in measurements of resonant harmonics [19]. Recently, multi-electron simulations [21] also confirmed the role of

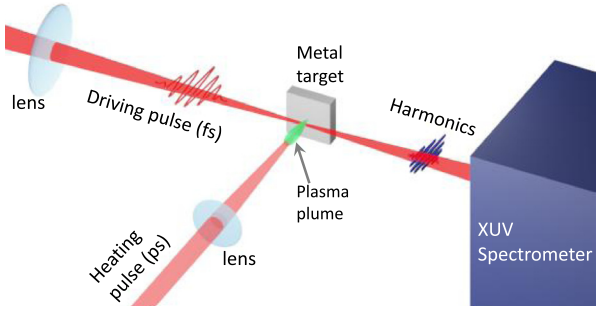

Fig. 1. Schematic diagram of experimental setup (see text).

autoionizing states in the process. A comprehensive review on the theoretical studies of resonant harmonics is given in [22].

However, most reported studies of resonant HHG in plasma plumes were performed with linearly polarized driving pulses, while the cases of elliptical polarization are mostly unexplored experimentally and theoretically. Although a linearly polarized field is generally the favorable choice for maximizing the probability of electron recollision and thus conversion efficiency, HHG with driving fields of elliptical polarization or other more complex polarization have attracted considerable research interest in recent years because they are relevant to the generation of isolated attosecond pulses [23] and elliptically polarized XUV radiation [24,25]. Classically, laser ellipticity serves as a sensitive knob for altering the sub-cycle dynamics of electrons, and therefore, studying how resonant harmonics vary with laser ellipticity may provide important clues that lead to a deeper understanding of the interplay between recollision dynamics and the resonance process of the system.

In this work, we investigate the driving laser ellipticity dependence of high harmonic yields in tin ions. We discuss the difference between the resonance-enhanced harmonic order and the other non-resonant orders. We also perform quantum mechanical simulations incorporating a single-active electron model of autoionizing resonance, and the results qualitatively reproduce the experimental observations. Our findings not only provide a new type of evidence for testing existing theories, but will also serve as an experimental reference for further theoretical development on resonant HHG with elliptically polarized lasers.

Our experiments use a 0.8 μm Ti:sapphire laser system (Spectra Physics: Spitfire Ace). It delivers two output beams: a 35 fs, 5.5 mJ beam and a 200 ps, 1.5 mJ beam (which is a split-off from the amplified beam before temporal compression). The experimental setup is schematically shown in Fig. 1. A metal target (tin or titanium) with a flat surface is located in a vacuum target chamber. The picosecond heating pulse is first focused at the target surface to form a laser-ablated plasma plume consisting of metal atoms and ions. Subsequently (after ~80 ns), the femtosecond driving pulse is focused at the plume to drive the HHG process. The polarization of the driving pulse is controlled by a quarter-wave plate. The harmonics are detected by a home-built XUV spectrometer located behind the target chamber [16]. The spectrometer consists of an entrance slit, a cylindrical mirror, a 1200 grooves/mm flat field grating, and a micro-channel plate (MCP) with a phosphor screen. The fluorescent signal on the phosphor screen is collected by a CCD camera.

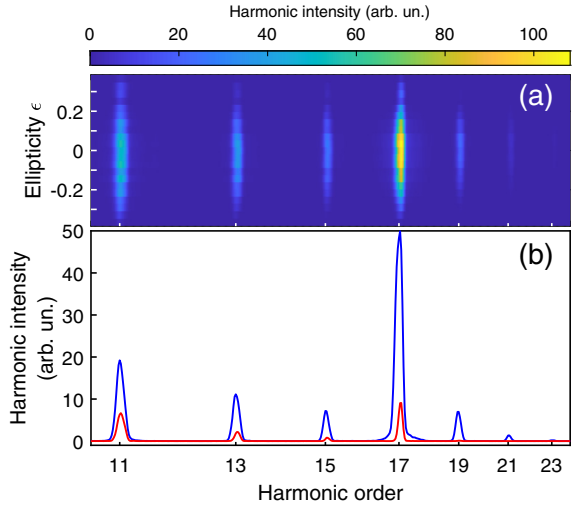

Fig. 2. HHG in plasma plume of tin. (a) Harmonic spectra as a function of driving ellipticity ϵ. (b) Harmonic spectra with linearly polarized (blue) and elliptically polarized ($\epsilon = 0.25$) driving fields (red).

We first consider the experimental data of tin. A total of 23 harmonic spectra generated at various driving ellipticities ϵ ranging from -0.35 to 0.35 are recorded. Ellipticity is defined as the ratio between the field amplitude of the two orthogonal components of the laser field. The driving intensity is kept constant, and it is estimated to be 2.4×10^{14} W/cm^2. All spectra are stacked together and presented as the 2D color plot in Fig. 2(a). It is observed that the yields of all harmonics decrease as the magnitude of ϵ increases from zero. For clarity, two of the spectra are plotted in Fig. 2(b), in which the blue and red lines are for $\epsilon = 0$ and $\epsilon = 0.25$, respectively. The enhanced 17th harmonic (H17) is clearly exhibited. While the overall harmonic yields in the case of the elliptically polarized driver are significantly lower than the case of the linearly polarized driver, H17 remains much stronger than the neighboring harmonics.

In Fig. 2(a), we extract the yield of each harmonic as a function of ϵ. Thus, to quantify the ϵ dependence of each harmonic order, Gaussian fits are applied to the yield versus ϵ data for each harmonic, and the half-width-at-half-maximum (HWHM) values of the fitted curve are obtained. Here, we refer to the fitted HWHM value as the threshold ellipticity ϵ_{th}. Physically, it represents the ellipticity value at which the generated harmonic yield is half of the yield in the case of a linearly polarized driving field. The fitted values of ϵ_{th} as a function of harmonic order are presented by the dots in Fig. 3. Except for H17, ϵ_{th} decreases monotonically with harmonic order.

The overall trend of decrease is in fact consistent with the properties of classical dynamics of electron recollision. We calculate the theoretical values of ϵ_{th} as a function of harmonic energy using the semiclassical formulation presented in [26], assuming that the measured harmonics are contributed mainly by the short quantum trajectories. In essence, the procedure is to first calculate the excursion times of the electron trajectories for each return energy and then evaluate the corresponding values of ϵ_{th} under the assumption that the distribution of initial transverse momentum of the electron $p_{\perp 0}$ is given by the Perelomov–Popov–Terent'ev (PPT) theory of strong-field ionization [27]. Two sets of calculated results are presented in Fig. 3, one is for harmonics generation from singly charged tin

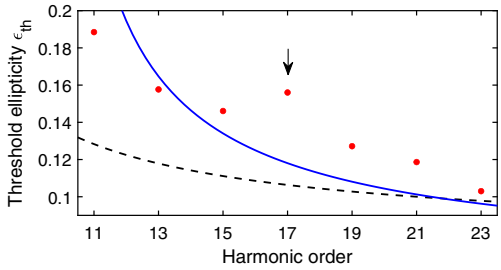

Fig. 3. Threshold ellipticity as a function of harmonic order in tin plasma. Dots: fitted values from the experiments. Predictions from classical calculations for tin atom and ion are shown by the dashed and solid lines, respectively.

ions (solid line), and the other is for neutral tin atoms (dashed line). Overall agreement between experiment and theory for ions is observed, and the fact that the agreement is better with the calculations for ion supports the assumption that the measured harmonics are indeed contributed mainly by the singly charged tin ions in the laser-ablated plume. In addition, from calculations of strong-field ionization probability, we also expect that ions of higher charge states would not significantly contribute to the measured spectrum. See Supplement 1 for supporting content.

From the results of tin shown in Fig. 3, we observe that the yield dependence of H17 on ellipticity deviates from the overall decreasing trend as a function of harmonic order. For comparison, we measure the ellipticity dependence of harmonic yields from a different target, titanium. It serves as a good reference target since its harmonic spectra are mostly featureless and without noticeable resonance effects. Figure 4(a) shows a spectrum generated by a linearly polarized laser. The procedure of harmonics measurement as a function of ellipticity and curve fitting is the same as the case of tin. The driving intensity is also similar (2.2×10^{14} W/cm^2). The fitted values of ϵ_{th} as a function of harmonic order are plotted in Fig. 4(b), and an overall decreasing trend without local maximum is observed.

We attempt to investigate whether our new experimental findings could be understood by the four-step model. For tin,

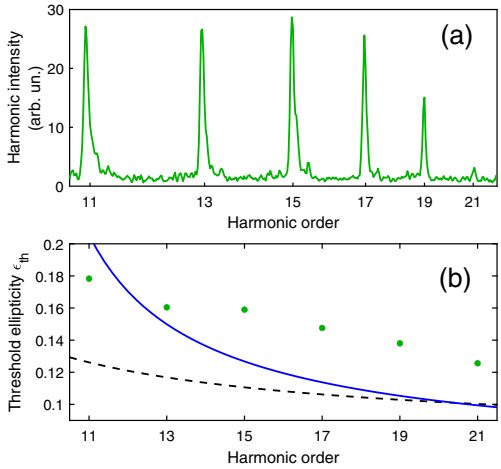

Fig. 4. HHG in plasma plume of titanium. (a) Harmonics spectra with linearly polarized driving field. (b) Threshold ellipticity as a function of harmonic order. Dots: fitted values from the experiments. Predictions from classical calculations for titanium atom and ion are shown by the dashed and solid lines, respectively.

the responsible autoionizing state for the enhancement of H17 is $4d^9 5s^2 5p^2 (^1D)^2 D_{5/2}$. So in this picture, the formation of enhancement relies on two factors: (i) the cross section for the electron recapture at the autoionizing state, and (ii) oscillator strength of the photo-transition between the ground and autoionizing states. The second factor is relatively well justified since oscillator strength is an intrinsic property of ions, and these values are accurately known. In strong-field processes, the a.c. Stark shift effect is often significant and should not be overlooked. However, that effect might not vary significantly as a function of driving ellipticity since the laser intensity is kept constant. On the other hand, the link between the first factor and the ellipticity dependence of the harmonics is more direct. To some extent, increasing the driving ellipticity is equivalent to increasing the impact parameter of the electron recollision process, which leads to a decrease in the probability of recapture. Heuristically, how quickly the probability drops as a function of the impact parameter should be related directly to the characteristic of the cross section for the recombination or recapture process.

To obtain theoretical predictions from the four-step model, we perform three-dimensional TDSE simulations for HHG (using the Qprop package [28]) with the model potential presented in [18], which was shown to be able to mimic the needed features of an autoionizing state within the single active electron approximation. The potential has the form of $V(r) = -2/\sqrt{a_0^2 + r^2} + a_1 \exp\{-[(r - a_2)/a_3]^2\}$ [29], in which the first term is a soft coulomb potential, and the second term forms a potential barrier that supports quasi-bound states with positive energy. The parameters are chosen to simulate a resonance at the energy of H17. Figure 5(a) shows a simulated harmonic spectrum generated by a linearly polarized driving field at a driving intensity of 2.4×10^{14} W/cm^2. A clearly enhanced H17 is produced as expected. Seven more simulations are run at different driving ellipticities, ranging between 0.05 and 0.35. All the spectra are stacked together and displayed in Fig. 5(b). Similar to the treatment with experimental data, here we extract the yields of each harmonic order from all the simulated spectra. We find that the yields decrease monotonically as a function of ellipticity. From these results, we again extract the values of ϵ_{th} for different harmonic orders, which are plotted in Fig. 5(c) together with the same classical calculation results (blue line) discussed in the previous section. A maximum at H17 is observed. Practically, due to the non-uniform intensity distribution of the focused laser beam, an experimentally measured spectrum does not purely represent the result from a single driving intensity. Therefore, we run a few more sets of simulations at different driving intensities (2.3, 2.6, and 2.9×10^{14} W/cm^2) to test the robustness of the existence of the maximum at H17 and find that a maximum ϵ_{th} value at H17 also appears in these cases. We do not find a maximum that persists for several different driving intensities at the same harmonic order when we perform TDSE simulations with a pure coulomb potential. Note that these simulations are based on a single atom response only and do not include any macroscopic effects.

If the rapidness of drop in the harmonic yields as a function of driving ellipticity indeed significantly depends on the spatial characteristic of the cross section for the recombination process, then the large value of ϵ_{th} for H17 in the simulations might be heuristically attributed to the fact that the spatial extent of the wave function of the autoionizing state is larger than that of the

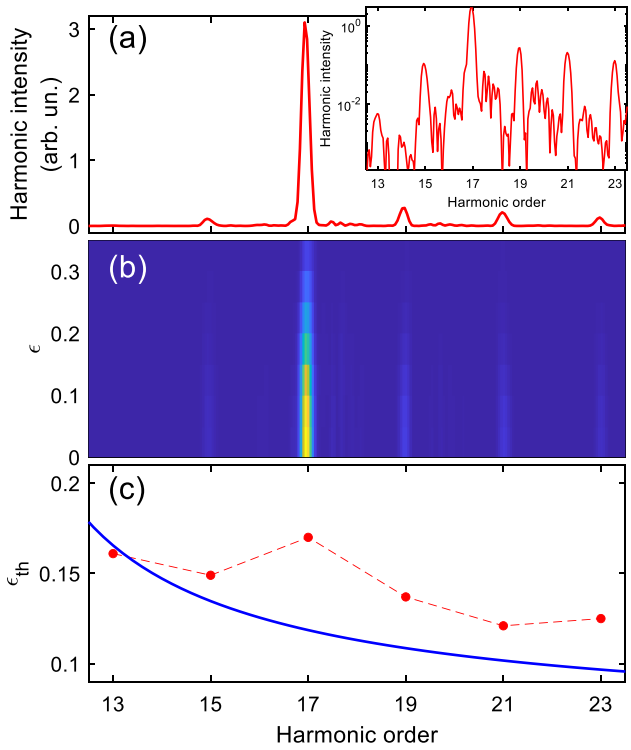

Fig. 5. TDSE simulations for resonant HHG. (a) Simulated harmonics spectrum with linearly polarized driving field. The inset shows the same spectrum, but the vertical axis has a logarithmic scale. (b) Simulated harmonic spectra as a function of driving ellipticity ϵ at a fixed driving intensity. (c) Values of ϵ_{th} extracted from the results in (b) are shown by dots. The solid line shows classical calculation result, which is the same as that in Fig. 3.

ground state in the model potential, which results in a larger wave function overlap between that state and the returning electron wave packet, and thus larger recombination probability under the same driving ellipticity. Although the simulations using a highly simplified single-electron model potential could be treated only as a qualitative reference, the success in reproducing a maximum of the ϵ_{th} values at H17 appears to suggest that our experimental results could be understood using the four-step model.

In summary, we have performed, to our knowledge, the first systematic investigation on the driving ellipticity dependence of resonance-enhanced high-harmonic yields in metal ions. We found that the resonance leads to a less rapid decay in yield as a function of driving ellipticity, and this feature is qualitatively reproduced by theoretical simulations in the framework of the four-step model [18]. To further elucidate the process, future investigations could focus on studying the driving ellipticity dependence of the harmonics ellipticity.

After the initial submission of this Letter, a theoretical investigation on the same subject by Khokhlova *et al.* was made available online [30].

Funding. National Natural Science Foundation of China (12004380); National Key Research and Development Program of China (2018YFB1107202); Strategic Priority Research Program of Chinese Academy of Sciences (XDA22010302); K. C. Wong Education Foundation (GJTD-2018–08).

Disclosures. The authors declare no conflicts of interest.

Data Availability. Data underlying the results presented in this paper are not publicly available at this time but may be obtained from the authors upon reasonable request.

Supplemental document. See Supplement 1 for supporting content.

REFERENCES AND NOTE

1. C.-D. Lin, C. Jin, A.-T. Le, and H. Wei, *Attosecond and Strong-field Physics: Principles and Applications* (Cambridge University, 2018).
2. M. Lewenstein, P. Balcou, M. Y. Ivanov, A. L'huillier, and P. B. Corkum, Phys. Rev. A **49**, 2117 (1994).
3. P. M. Paul, T. O. Clatterbuck, C. Lyngå, P. Colosimo, L. F. DiMauro, P. Agostini, and K. C. Kulander, Phys. Rev. Lett. **94**, 113906 (2005).
4. X. Yuan, P. Wei, C. Liu, Z. Zeng, Y. Zheng, J. Jiang, X. Ge, and R. Li, Appl. Phys. Lett. **107**, 041110 (2015).
5. J. Rothhardt, S. Hädrich, S. Demmler, M. Krebs, S. Fritzsche, J. Limpert, and A. Tünnermann, Phys. Rev. Lett. **112**, 233002 (2014).
6. A. D. Shiner, B. E. Schmidt, C. Trallero-Herrero, H. J. Wörner, S. Patchkovskii, P. B. Corkum, J. C. Kieffer, F. Légaré, and D. M. Villeneuve, Nat. Phys. **7**, 464 (2011).
7. M. A. Fareed, V. V. Strelkov, M. Singh, N. Thiré, S. Mondal, B. E. Schmidt, F. Légaré, and T. Ozaki, Phys. Rev. Lett. **121**, 023201 (2018).
8. R. A. Ganeev, M. Suzuki, M. Baba, H. Kuroda, and T. Ozaki, Opt. Lett. **31**, 1699 (2006).
9. M. Suzuki, M. Baba, H. Kuroda, R. A. Ganeev, and T. Ozaki, J. Opt. Soc. Am. B **24**, 2686 (2007).
10. R. Ganeev, S. Odžak, D. Milošević, M. Suzuki, and H. Kuroda, Laser Phys. **26**, 075401 (2016).
11. L. Elouga Bom, F. Bouzid, F. Vidal, J. Kieffer, and T. Ozaki, J. Phys. B **41**, 215401 (2008).
12. I. A. Kulagin and T. Usmanov, Opt. Lett. **34**, 2616 (2009).
13. R. A. Ganeev, T. Witting, C. Hutchison, V. V. Strelkov, F. Frank, M. Castillejo, I. Lopez-Quintas, Z. Abdelrahman, J. W. G. Tisch, and J. P. Marangos, Phys. Rev. A **88**, 033838 (2013).
14. N. Rosenthal and G. Marcus, Phys. Rev. Lett. **115**, 133901 (2015).
15. M. Fareed, V. Strelkov, N. Thiré, S. Mondal, B. Schmidt, F. Légaré, and T. Ozaki, Nat. Commun. **8**, 16061 (2017).
16. J. Liang, M. Venkatesh, G. S. Boltaev, R. A. Ganeev, Y. H. Lai, and C. Guo, Atoms **9**, 1 (2021).
17. D. Milošević, J. Phys. B **40**, 3367 (2007).
18. V. Strelkov, Phys. Rev. Lett. **104**, 123901 (2010).
19. S. Haessler, V. Strelkov, L. B. E. Bom, M. Khokhlova, O. Gobert, J.-F. Hergott, F. Lepetit, M. Perdrix, T. Ozaki, and P. Salières, New J. Phys. **15**, 013051 (2013).
20. V. V. Strelkov, M. A. Khokhlova, and N. Y. Shubin, Phys. Rev. A **89**, 053833 (2014).
21. I. S. Wahyutama, T. Sato, and K. L. Ishikawa, Phys. Rev. A **99**, 063420 (2019).
22. G. S. Armstrong, M. A. Khokhlova, M. Labeye, A. S. Maxwell, E. Pisanty, and M. Ruberti, "Dialogue on analytical and ab initio methods in attoscience," arXiv preprint arXiv:2101.09335 (2021).
23. M. Chini, K. Zhao, and Z. Chang, Nat. Photonics **8**, 178 (2014).
24. A. Fleischer, O. Kfir, T. Diskin, P. Sidorenko, and O. Cohen, Nat. Photonics **8**, 543 (2014).
25. P.-C. Huang, C. Hernández-García, J.-T. Huang, P.-Y. Huang, C.-H. Lu, L. Rego, D. D. Hickstein, J. L. Ellis, A. Jaron-Becker, A. Becker, S.-D. Yang, C. G. Durfee, L. Plaja, H. C. Kapteyn, M. M. Murnane, A. H. Kung, and M.-C. Chen, Nat. Photonics **12**, 349 (2018).
26. V. V. Strelkov, M. A. Khokhlova, A. A. Gonoskov, I. A. Gonoskov, and M. Y. Ryabikin, Phys. Rev. A **86**, 013404 (2012).
27. A. Perelomov, V. Popov, and M. Terent'ev, Sov. Phys. JETP **23**, 924 (1966).
28. V. Tulsky and D. Bauer, Comput. Phys. Commun. **251**, 107098 (2020).
29. $a_0 = 0.435$; $a_1 = 0.9$; $a_2 = 3.4$; $a_3 = 2.5$.
30. M. A. Khokhlova, M. Y. Emelin, M. Y. Ryabikin, T. Sato, K. L. Ishikawa, and V. V. Strelkov, "Polarisation control of quasi-monochromatic XUV produced via resonant high harmonic generation," arXiv preprint arXiv:2102.05071 (2021).